Absence of Platinum Enhancement of a Photoreaction on TiO_2−CO Photooxidation on $Pt/TiO_2(110)$

Amy Linsebigler, Camelia Rusu, and John T. Yates, Jr.*

Contribution from the Surface Science Center, Department of Chemistry, University of Pittsburgh, Pittsburgh, Pennsylvania 15260

Received October 27, 1995[⊗]

Abstract: The influence of deposited Pt metal clusters on the CO photooxidation reaction on the $TiO_2(110)$ surface was investigated. An enhancement in the CO photooxidation reaction rate or yield is not observed in the presence of Pt metal clusters on the $TiO_2(110)$ surface. These results indicate that kinetic models involving Schottky-barrier electron trapping in metal deposits leading to enhanced electron-hole pair lifetimes are not applicable in the case of CO photooxidation on $Pt/TiO_2(110)$.

I. Introduction

Numerous investigations have reported that the addition of group VIII metals to high-surface-area powdered TiO_2-based photocatalytic systems enhances the photocatalytic activity.[1−8] The most active metal for photocatalytic enhancement is platinum. The Pt/TiO_2 photocatalysts were probed by monitoring the enhanced yield and/or rate obtained for intermediates or products and/or the difference in selectivity for product formation with a varying level of added metal. It is postulated that the Pt clusters present on the TiO_2 surface capture the excited electrons in the TiO_2 conduction band produced by band gap (3.1 eV) excitation. Platinum should produce a large enhancement in photocatalytic activity for TiO_2 because, within the framework of the hypothesis, it possesses the highest work function. Platinum therefore produces the highest Schottky barrier among the metals facilitating the electron capture. The capture of the electrons by the Pt is postulated to produce a longer electron-hole pair separation lifetime and therefore to facilitate enhanced transfer of holes and possibly electrons to the reactants adsorbed on the TiO_2 surface. It has been found that the presence of Pt enhances H_2 formation in the photocatalytic degradation of organic species.[1−3,7]

In contrast to the previous investigations of the role of Pt on the photocatalytic activity of high-area TiO_2 powders, this investigation was carried out on the $TiO_2(110)$ single-crystal surface where the atomic structure, surface cleanliness, and defect density could be controlled using surface science methods on atomically clean surfaces in ultrahigh vacuum. Such methods provide a more definitive view of the fundamental surface conditions present in model TiO_2-based photocatalysts.[3]

In the present report, quantitative studies of CO photooxidation on $TiO_2(110)$ and $Pt/TiO_2(110)$ are presented. The studies are performed at low temperature where thermal reactions will be quenched, allowing electronic effects to be more clearly studied. The results demonstrate how the addition of Pt, in different morphological states, to the $TiO_2(110)$ surface does not enhance the kinetic rate or yield for the photooxidation reaction of CO. This finding is contrary to a report that CO photooxidation rates are significantly enhanced by electron trapping in Pt on Pt/TiO_2/pillared montmorillonite clay photocatalysts.[8]

II. Experimental Section

A. Apparatus. The experiments reported here were performed in a stainless steel vacuum (UHV) chamber described in detail elsewhere.[9−11] The chamber is equipped with the following: (1) a shielded and apertured UTI 100C quadrupole mass spectrometer (QMS) for temperature-programmed desorption (TPD) measurements;[12] (2) a Perkin-Elmer digitally controlled cylindrical mirror analyzer (CMA) for Auger electron spectroscopy (AES) analysis; (3) an ion gun for Ar^+ sputter cleaning; (4) a home-built low-energy electron-diffraction (LEED) apparatus containing two microchannel plates for amplification; (5) a shielded Pt evaporator source;[10] (6) a rotatable temperature-controlled quartz oscillator thickness monitor (QTM) for accurate Pt flux calibration;[10] (7) a collimated and calibrated microcapillary array doser for accurate gas exposure to the crystal surface;[13−16] and (8) an external high-pressure Hg lamp (Oriel) with an interference filter which passes photons of 3.94 ± 0.07 eV energy, used for the photooxidation experiments. A photon flux of 1.8×10^{15} photons/(cm^2•s) is employed in the experiments reported here as measured with a photodiode. The temperature of the crystal increased by <1 K while using UV radiation.

B. Crystal Preparation. A polished ($10 \times 10 \times 1$ mm) $TiO_2(110)$ single crystal was obtained from Commercial Crystal Laboratories, Inc. The crystal was oriented to within $\pm 0.5°$ of the (110) plane as determined by Laue back-reflection X-ray studies. The crystal was mounted onto a Ta support plate (of the same dimension as the crystal) with Ta clips.[17] The mounting allowed for direct sampling of the front face of the crystal during thermal and photodesorption

[⊗] Abstract published in *Advance ACS Abstracts,* May 1, 1996.

(1) Grätzel, M. *Hetergeneous Photochemical Electron Transfer;* CRC Press: Boca Raton, 1989, and references therein.
(2) Fox, M. A.; Dulay, M. T. *Chem. Rev.* **1993**, *93*, 341 and references therein.
(3) Linsebigler, A. L.; Lu, G.; Yates, J. T., Jr. *Chem. Rev.* **1995,** *95*, 735 and references therein.
(4) Kraeutler, B.; Bard, A. J. *J. Am. Chem. Soc.* **1978**, *100*, 5985.
(5) Izumi, I.; Dunn, W. W.; Wilbourn, K. O.; Fan, F.-R. F.; Bard, A. J. *J. Phys. Chem.* **1980**, *84*, 3207.
(6) Izumi, I.; Fan, F.-R. F.; Bard, A. J. *J. Phys. Chem.* **1981**, *85*, 218.
(7) St. John, M. R.; Furgala, A. J.; Sammells, A. F. *J. Phys. Chem.* **1983**, *87*, 801.
(8) Takahama, K.; Sako, T.; Yokoyama, M.; Hirao, S. *Nippon Kagaku Kaishi* **1994**, *7*, 613.
(9) Lu, G.; Linsebigler, A. L.; Yates, J. T., Jr. *J. Vac. Sci. Technol. A* **1994**, *12(2)*, 384.
(10) Linsebigler, A. L.; Lu, G.; Yates, J. T., Jr. *Surf. Sci.* **1993**, *294*, 284.
(11) Hanley, L.; Guo, X.; Yates, J. T., Jr. *J. Chem. Phys.* **1989**, *91*, 7220.
(12) Lu, G.; Linsebigler, A. L.; Yates, J. T., Jr. *J. Vac. Sci. Technol. A* **1994**, *12*, 384.
(13) Bozack, M. J.; Muehlhoff, L.; Russell, J. N., Jr.; Choyke, W. J.; Yates, J. T., Jr.; *J. Vac. Sci. Technol. A.* **1987**, *5*, 1.
(14) Winkler, A.; Yates, J. T., Jr. *J. Vac. Sci. Technol. A* **1988**, *6*, 2929.
(15) Campbell, C. T.; Valone, S. M. *J. Vac. Sci. Technol. A* **1985**, *3*, 408.
(16) Linsebigler, A. L.; Smentkowski, V. S.; Ellison, M. D.; Yates, J. T., Jr. *J. Am. Chem. Soc.* **1992**, *114*, 465.
(17) Lu, G.; Linsebigler, A. L.; Yates, J. T., Jr. *J. Chem. Phys.* **1995**, *102*, 4657.

S0002-7863(95)03601-8 CCC: $12.00

measurements. The Ta support was cooled and resistively heated through two 0.35-mm-diameter tungsten wires spot welded to its back. The wires were in turn welded to two 1.0-mm-diameter tungsten rods. The whole assembly, electrically isolated by sapphire wafers from the OFHC Cu cooling posts, was cooled with liquid nitrogen. The Ta support plate provided thermal contact and allowed the crystal to reach temperatures as low as 100 K. The temperature of the crystal was measured by a type-K thermocouple inserted into a precut slot at one corner of the crystal. The thermocouple was positioned against the inner wall of the slot with a high-temperature ceramic adhesive (AREMCO 571) which has nearly the same thermal conductivity and thermal expansion coefficient as TiO_2. This method of measuring the TiO_2 crystal temperature directly, rather than the temperature of a metal support in contact with the crystal, is likely to provide a more correct measurement of the TiO_2 temperature. The thermocouple feedback to the temperature controller permitted linear heating of the crystal between 100 and 1000 K.[18] The heating rate employed for this work in both the crystal annealing procedure and in TPD measurements was 0.5 K/s.

The crystal was initially cleaned to remove potassium, calcium, sulfur, and carbon by successive intervals of sputtering and annealing to 900 K. The stoichiometric (oxidized) surface was obtained by annealing the clean surface in an $^{16}O_2$ flux (6.9×10^{12} molecules/(cm^2·s)) to 900 K momentarily, followed by continuous exposure to O_2 at 300 K for at least 1 h. The surface thus prepared yielded a sharp (1×1) LEED pattern. The surface defects (oxygen vacancies) were produced by annealing the above surface in vacuum to 900 K momentarily, and it was shown that the controlled annealing procedure yielded reproducible results indicative of the presence of a reproducible coverage of vacancy defects. This reproducibility in defect surface density was demonstrated by ultraviolet photoemission spectroscopy (UPS),[19−21] X-ray photoemission spectroscopy (XPS),[19,21,22] ion scattering spectroscopy (ISS),[19] and chemisorption experiments.[23] The ISS study[19] has given an upper limit of ∼0.08 ML (ML = monolayer) of oxygen vacancies on the annealed TiO_2(110) surface. Photodesorption measurements of $^{18}O_2$ from the defect sites of TiO_2(110) have measured a defect density of ∼0.12 ML.[17] Here a monolayer is defined as the number of Ti and O atoms on TiO_2 (110), 2.1×10^{15} per cm^2.

C. Pt Source Calibration. Detailed information on the calibration and deposition of Pt has been reported elsewhere.[10] Briefly, the Pt source consists of Pt wire (99.998% pure) wound around a tungsten filament supported by two degassing loops. The loops can be degassed independently by ohmic heating to reduce the evolution of impurity gases to a very low level when the Pt is being evaporated. The QTM (Sycon Instruments) was mounted on a rotatable flange and could be moved to three positions to allow for Pt source outgassing, calibration by Pt deposition on the QTM, and Pt deposition on the TiO_2 crystal. The temperature of the QTM was maintained constant to ±0.5 K during Pt deposition using a water thermostat. The QTM was used to calibrate the flux from the Pt source before and after deposition on the TiO_2(110) crystal in order to determine an accurate deposition rate. The deposition rate typically changes by less than ±4% during the deposition of several monolayers. It is estimated from calibration experiments and from an analysis of the systematic geometrical errors that the deposited *absolute* Pt coverage can be determined to ±16% in the submonolayer regime.[10]

D. Gas Adsorption. The surface was dosed separately with isotopically labeled carbon monoxide ($C^{18}O$) and oxygen ($^{18}O_2$) through the microcapillary array collimated beam doser. The conductance of the beam doser was controlled by a pinhole aperture.[13−16] The beam doser was calibrated with N_2 using standard volumetric methods and exhibited a conductance of $(2.64 \pm 0.26) \times 10^{13}$ N_2/(torr·s). Based on the geometrical arrangement, a geometrical fractional interception of 0.3 was estimated when the crystal was placed in the dosing position.[14] For multiple gas exposures, each gas was independently dosed at a crystal temperature of 105 K, with O_2 being dosed first. The carbon monoxide ($C^{18}O$) was obtained from MSD Isotopes (97.8 atomic % ^{18}O). The isotopically labeled $^{18}O_2$ was obtained from Cambridge Isotopes; with an isotopic purity of 98+ atomic % ^{18}O.

In all of the CO plus O_2 coadsorption experiments reported here, standard fluences of O_2 and CO were employed. The annealed crystal was exposed first to 1.4×10^{15} O_2/cm^2 at 105 K, then to 2.5×10^{14} CO/cm^2 at 105 K.

E. Thermal and Photodesorption Measurements. To perform the thermal and photodesorption measurements, the crystal was positioned line-of-sight in front of the aperture at the differentially pumped mass spectrometer shield.[17] The crystal temperature was increased at a linear rate in this position for thermal desorption measurements. For photodesorption measurements, the light from the photon source entered at a 60° angle to the surface normal. The surface normal was aligned parallel to the mass spectrometer axis (line-of-sight configuration). The mounting and surface configuration prevented sampling of gases desorbing from the support.

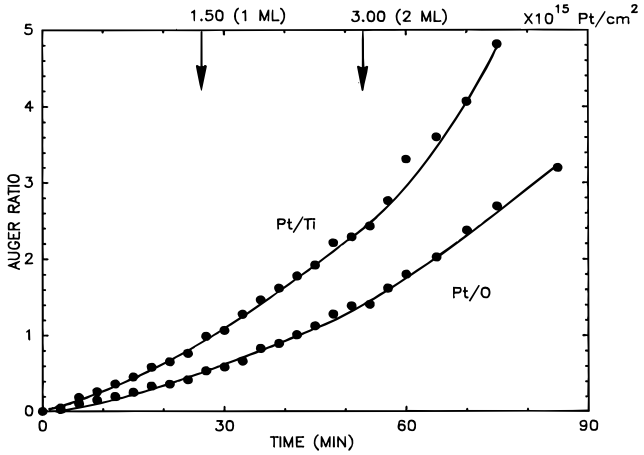

Figure 1. Plot of the Pt(NVV)/Ti(LMM) and Pt(NVV)/O(KLL) Auger ratios as a function of the deposition time of Pt atoms at a substrate temperature of 300 K. The absolute coverage of Pt is labeled on the top horizontal axis, as determined by quartz microbalance methods. Monolayer coverage is assumed to correspond to the close packing density of Pt atoms on Pt (111), namely 1.50×10^{15} Pt/cm^2.

III. Results

A. Characterization of Pt Deposition and Thermal Stability. After calibrating the Pt flux with the QTM, Auger electron spectroscopy was used to monitor the growth of Pt layers on the TiO_2(110) surface at 300 K. The TiO_2(110) crystal surface was dosed with Pt for 3-min increments in the line-of-sight position. The crystal was rotated in front of the CMA and an Auger spectrum was obtained using a 1.5 kV electron beam current of $(1.0 \pm 0.05) \times 10^{-6}$ A. The procedure was then repeated until completion of the deposition curve presented in Figure 1. The Pt(NVV)/Ti(LMM) ratio and the Pt(NVV)/O(KLL) ratios are plotted as a function of deposition time. The Auger ratio curves slope upward as expected for deposition, but the data do not permit a growth mode to be determined. A (1×1) LEED pattern for Pt(111) was obtained at coverages >3 ML. One monolayer (ML) of deposited Pt is assumed to be 1.5×10^{15} Pt/cm^2, the close packing density of Pt on the Pt(111) surface.

CO thermal desorption measurements were obtained as a function of Pt coverage. Spectrum A in Figure 2 shows the CO thermal desorption spectrum from a clean TiO_2(110) surface in the presence of coadsorbed O_2 after dosing with a saturation exposure of CO. The CO desorbs from the surface with a T_{max} = ∼140 K.[24] Spectrum B illustrates the CO thermal desorption from a 0.15 ML Pt-covered TiO_2(110) surface. The Pt was

(18) Muha, R. J.; Gates, S. M.; Basu, P.; Yates, J. T., Jr. *Rev. Sci. Instrum.* **1985**, *56*, 613.

(19) Pan, J.-M.; Maschhoff, B. L.; Diebold, U.; Madey, T. E. *J. Vac. Sci. Technol. A* **1992**, *10*, 2470.

(20) Kurtz, R. L.; Stockbauer, R.; Madey, T. E.; Roman, E.; de Segovia, J. L. *Surf. Sci.* **1989**, *218*, 178.

(21) Göpel, W.; Rocker, G.; Feierabend, R. *Phys. Rev. B* **1983**, *28*, 3427.

(22) Göpel, W.; Anderson, J. A.; Frankel, D.; Jaehnig, M.; Phillips, K.; Schafer, J. A.; Rocker, G. *Surf. Sci.* **1984**, *139*, 133.

(23) Lu, G.; Linsebigler, A. L.; Yates, J. T., Jr. *J. Phys. Chem.* **1994**, *98*, 11733.

(24) Linsebigler, A. L.; Lu, G.; Yates, J. T., Jr. *J. Chem. Phys.* **1995**, *103*, 9438.

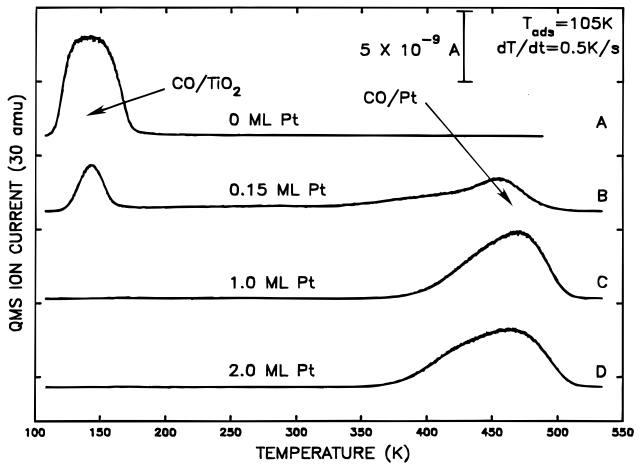

Figure 2. Temperature-programmed desorption spectra of $C^{18}O$ co-adsorbed with O_2 from (A) a clean TiO_2(110) surface; (B) a 0.15-ML Pt layer deposited on the TiO_2(110) surface at 300 K; (C) a 1-ML Pt layer deposited on the TiO_2(110) surface at 300 K; and (D) a 2-ML Pt layer deposited on the TiO_2(110) surface at 300 K.

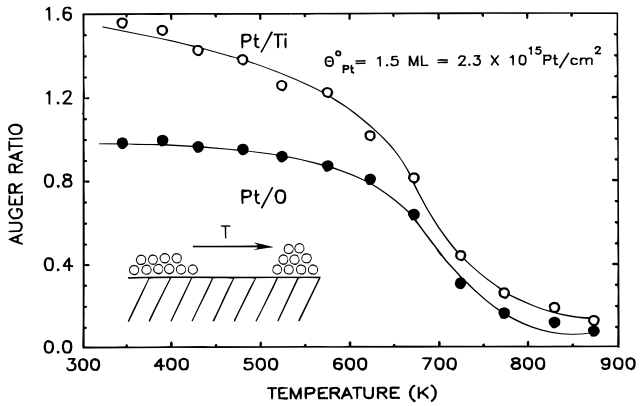

Figure 3. Plot of the Pt(NVV)/Ti(LMM) and Pt(NVV)/O(KLL) Auger ratios as a function of annealing temperature for a 1.5-ML Pt film deposited at 300 K. The formation of Pt clusters is schematically indicated.

deposited at 300 K. The spectrum shows a reduction in the CO thermal desorption process from the TiO_2(110) surface at $T \sim 140$ K and an additional CO desorption peak at ~460 K, which is caused by CO thermal desorption from Pt. This peak temperature is in agreement with CO thermal desorption from Pt single-crystal surfaces.[25−27] The CO thermal desorption spectrum from 1 ML of deposited Pt shows the complete elimination of the CO thermal desorption process from the TiO_2(110). The only thermal desorption peak observed is attributed to CO thermal desorption from Pt. Spectrum D shows the thermal desorption spectrum for CO from 2 ML of deposited Pt, which is in agreement with the CO thermal desorption process for 1 ML of deposited Pt.

The Pt(NVV)/Ti(LMM) and Pt(NVV)/O(KLL) Auger ratios were monitored as a function of annealing temperature for a Pt coverage of 1.5 ML deposited at 300 K and the data are shown in Figure 3. The surface was heated in temperature increments of 50 K, where the temperature was stabilized and an Auger spectrum was obtained at each temperature. The Auger ratios remained constant after the crystal was cooled to 300 K (i.e., the thermal behavior is not reversible). As the temperature of the surface was increased there was a slow reduction in the Pt/Ti and Pt/O Auger ratios up to 600 K. This decrease is

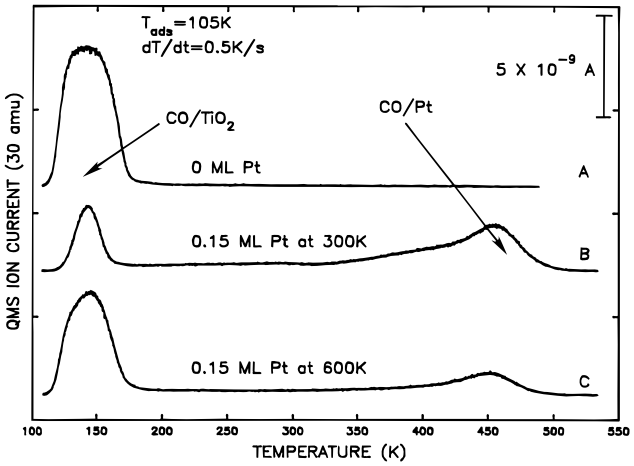

Figure 4. Temperature-programmed desorption spectra of ^{18}CO co-adsorbed with O_2 from (A) a clean TiO_2(110) surface, (B) a 0.15-ML Pt layer deposited on the TiO_2(110) surface at 300 K; and (C) the Pt layer in (B) annealed to 600 K. Saturation CO exposure = 2.5×10^{14} molecules/(cm^2·s).

attributed to clustering of Pt which decreases the Pt signal due to attenuation of Auger intensity from the underlayers in the Pt clusters. At temperatures above 600 K the Auger ratios decrease significantly and at $T > 800$ K, the Auger ratios remained relatively constant up to 900 K. The same fractional change in the Auger ratio for particular annealing temperatures for different coverages up to 4 ML of Pt was observed for the annealing process. It has previously been proposed that in the temperature range 750−900 K, further clustering occurs along with migration of Ti_xO_y over the Pt clusters.[28]

CO thermal desorption measurements were also conducted as a function of annealing temperature for the Pt-covered TiO_2(110) surface. Spectrum A in Figure 4 shows the CO thermal desorption spectrum from a clean TiO_2(110) surface, as in Figure 2. Spectrum B illustrates the CO thermal desorption spectrum from a Pt-covered TiO_2(110) surface containing 0.15 ML of Pt deposited at a TiO_2 temperature of 300 K. The spectrum shows a reduction in the CO thermal desorption process from the TiO_2(110) surface at $T \sim 140$ K and an additional CO desorption peak at ~460 K, which is caused by CO thermal desorption from Pt. Spectrum C shows the CO thermal desorption spectrum from the 0.15-ML Pt-covered TiO_2(110) surface after it was annealed to 600 K. Spectrum C shows a reduction in the CO peak at ~460 K attributed to desorption from Pt and an increase in the CO thermal desorption peak from the TiO_2(110) surface at ~150 K. This confirms the conclusion based on Auger spectroscopy (Figure 3) that as the Pt-covered TiO_2(110) surface is annealed to high temperatures, the Pt metal forms clusters which reduce the surface area for CO adsorption on Pt and increase the surface area for CO adsorption on the TiO_2(110) surface. The total thermal desorption yield of CO for all three experiments was essentially constant.

CO thermal desorption measurements were also conducted for thick Pt layers on the TiO_2(110) surface as a function of annealing temperature. As the surface is annealed to increasing temperatures, the CO thermal desorption peak at ~460 K shifts to lower temperatures. When the Pt-covered surface is annealed to $T > 800$ K, CO does not adsorb on the Pt surface. As stated previously, it is believed that Ti_xO_y migrates over and encapsulates the Pt clusters at temperatures above ~750 K.[28]

In order to investigate the hypothesis that Ti_xO_y migration on top of the Pt clusters occurs above 800 K, low flux sputtering

(25) Avery, N. R. *J. Chem. Phys.* **1981**, *74*, 4202.
(26) Szabo, A.; Kiskinova, M.; Yates, J. T., Jr. *J. Chem. Phys.* **1989**, *90*, 4604.
(27) Siddiqui, H. R.; Guo, X.; Chorkendorff, I.; Yates, J. T., Jr.. *Surf. Sci.* **1987**, *191*, L813.
(28) Belton, D. N.; Sun, Y.-M.; White, J. M. *J. Phys. Chem.* **1984**, *88*, 1690. Sun, Y.-M.; Belton, D. N.; White, J. M. *J. Phys. Chem.* **1986**, *90*, 5178.

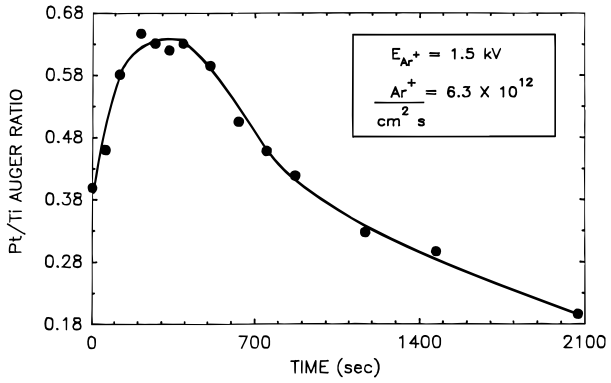

Figure 5. The Pt(NVV)/Ti(LMM) Auger ratio as a function of sputtering time for a 2-ML Pt-covered surface annealed to 900 K where Ti_xO_y encapsulates the Pt clusters. The curve maximum at 300 s corresponds to an Ar^+ fluence of ~1 ML, assuming 2×10^{15} Ar^+/cm^2 = 1 ML.

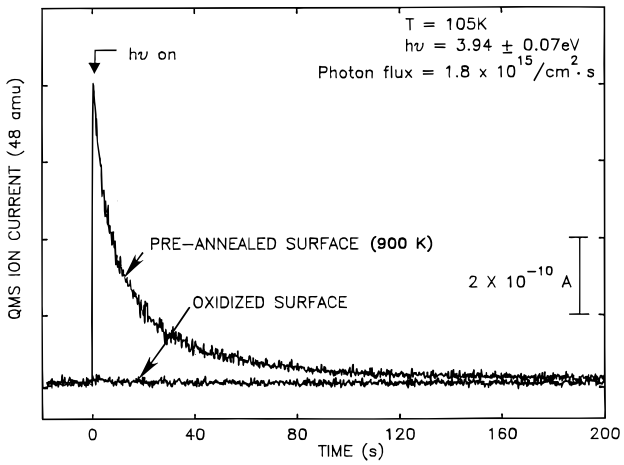

Figure 6. A comparison of the photoformation of $^{18}CO_2$ from the preannealed $TiO_2(110)$ surface (containing vacancy defect sites) to the oxidized $TiO_2(110)$ surface (where vacancy defect sites are absent) where no photoformation of CO_2 is observed.

measurements were made. Figure 5 illustrates the Pt/Ti Auger ratio as a function of sputtering time for a Pt-covered surface annealed to 900 K (the Pt/O Auger ratio exhibits the same behavior). The figure illustrates that at short sputtering times, the Pt/Ti Auger ratio increases. This experiment confirms that the Ti_xO_y has migrated at 900 K over the Pt clusters and that during a short sputtering time the Pt clusters are uncovered.

B. CO Photooxidation on the Annealed $TiO_2(110)$ Surface. The photooxidation of CO with molecular oxygen is only observed when the $TiO_2(110)$ surface is preannealed to $T >$ 400 K to produce oxygen vacancy sites (Ti^{3+} sites). The fully oxidized or stoichiometric $TiO_2(110)$ surface is inert for the photooxidation of CO with molecular oxygen.[29] The bottom curve of Figure 6 exhibits no measurable signal for 48 amu ($C^{18}O_2$) when the oxidized surface is exposed to UV radiation after $^{18}O_2$ and $C^{18}O$ exposure. The top curve of Figure 6 illustrates the rapid photodesorption of $C^{18}O_2$ when the shutter for the light source is opened to expose the pre-annealed surface (900 K) containing a mixture of chemisorbed $C^{18}O$ and $^{18}O_2$. The photodesorption trace reached a maximum within the time resolution of our measurements (0.2 s) and then decayed as reactant CO and O_2 were consumed. For this particular experiment the $TiO_2(110)$ surface was pre-annealed to 900 K prior to $^{18}O_2$ exposure at 105 K, followed by $C^{18}O$ exposure at 105 K. Molecular oxygen chemisorbs at the defect sites

(29) Linsebigler, A. L.; Lu, G.; Yates, J. T., Jr. *J. Phys. Chem.* **1996**, *100*, 6631.

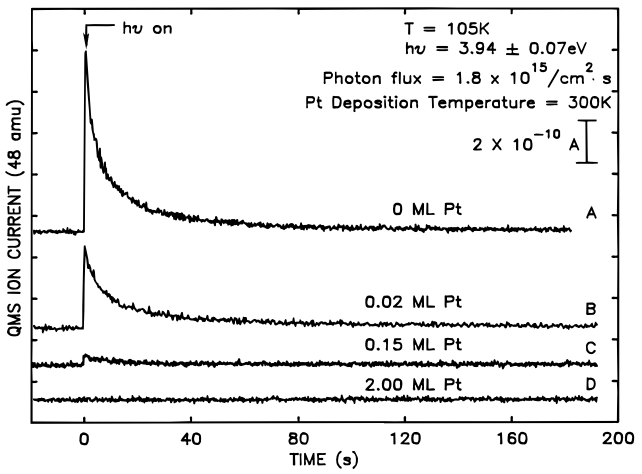

Figure 7. The photoformation of CO_2 from chemisorbed CO and O_2 for various coverages of Pt on the $TiO_2(110)$ surface up to 2 ML. Pt deposition temperature = 300 K, where little 3-D Pt cluster formation occurs.

produced from annealing the surface to 900 K to a saturation coverage of 0.12 ML.[17] Therefore, the comparison in Figure 6 shows that molecular oxygen is not active for photoreaction with CO unless adsorbed at oxygen vacancy sites.

C. The Effect of Deposited Pt on the CO Photooxidation Reaction. The behavior of Pt and chemisorbed CO demonstrated previously provides a basis for a controlled experiment to detect the hypothesized role of Pt as an electron trap in the photooxidation of CO on the $Pt/TiO_2(110)$ model surface. Figure 7 shows the CO_2 photoformation on $TiO_2(110)$ as a function of Pt coverage where Pt clustering has not been purposely carried out by annealing. Spectrum A is the typical CO_2 photodesorption signal from an O_2 and CO mixture on the clean $TiO_2(110)$ surface which was previously annealed to 900 K to produce surface defects. Figure 7 shows that as the Pt coverage is increased on the defective $TiO_2(110)$ surface (spectra B, C, and D), the yield of photoformed CO_2 is reduced. The CO_2 signal is almost completely eliminated at a Pt coverage of 0.15 ML. This coverage is in close agreement with the measured oxygen vacancy density on the $TiO_2(110)$ surface of 0.12 ML.[17] The results illustrate that as Pt is deposited on the surface at 300 K, it titrates the defect sites eliminating the CO photooxidation reaction. Figure 7D also shows that photocatalytic oxidation of CO does not occur on a 2 ML Pt film on $TiO_2(110)$.

The morphology of Pt in high-area, powdered Pt/TiO_2 photocatalysts is usually in the form of clusters.[1−8] Therefore, the CO photooxidation reaction was also carried out on the 600 K annealed Pt-covered $TiO_2(110)$ surface. Heating of the Pt-covered surface to cause Pt clustering at 600 K also regenerates oxygen vacancy defect sites on the exposed regions of the $TiO_2(110)$ surface. Spectrum A of Figure 8 illustrates the CO_2 photoformation from a clean $TiO_2(110)$ surface annealed to 600 K. This spectrum provides a calibration of the CO_2 photoproduction yield from the defect density present after 600 K annealing of the $TiO_2(110)$ surface. Spectrum B shows the CO_2 photoformation after Pt deposition at 300 K to a coverage of 0.15 ML. As indicated previously, this coverage of Pt almost completely titrates the oxygen vacancy sites, reducing the rate of CO_2 production and the yield of CO_2. Spectrum C illustrates the CO_2 photoformation after the 0.15 ML Pt-covered surface was annealed to 600 K causing Pt clustering. This results in the production of TiO_2 vacancy defect sites. Even though the CO_2 yield increased on the surface, which was annealed to 600 K, the CO_2 photoformation rate (measured by the initial CO_2 peak height) and the total yield

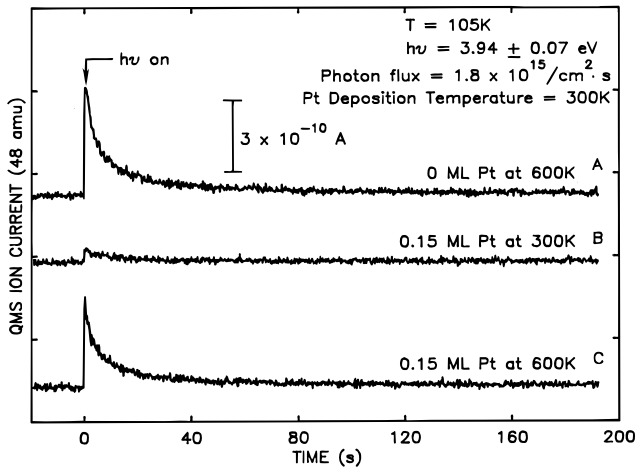

Figure 8. A comparison of the photoformation of CO_2 from (A) a clean TiO_2(110) surface annealed to 600 K and from (B) 0.15 ML of Pt deposited on the TiO_2(110) surface at 300 K and (C) annealed to 600 K to form 3-D Pt clusters, exposing the TiO_2 surface containing vacancy defect sites.

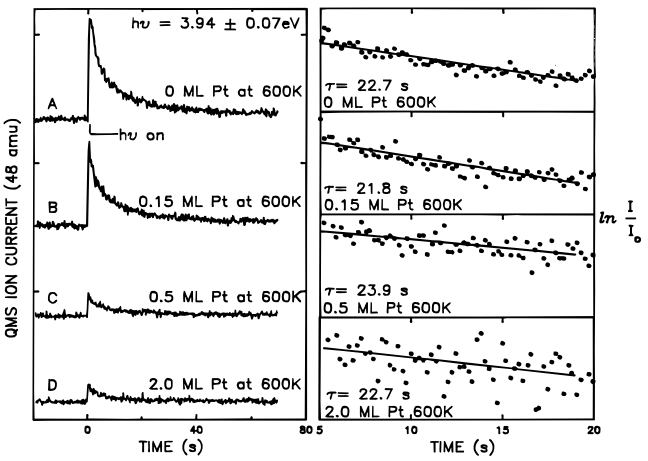

Figure 9. Kinetics of CO_2 production for CO + O_2 layers on TiO_2(110) containing various coverages of Pt. The surface is annealed to 600 K to produce 3-D Pt clusters as well as vacancy defect sites on exposed TiO_2 regions. Left panel: rate of CO_2 formation. Right panel: characteristic decay time for CO_2 formation reaction evaluated after 2.5 s of irradiation.

(measured by the CO_2 peak area) do not show an enhancement compared to the clean TiO_2(110) surface.

The left panel of Figure 9 illustrates that even when higher coverages of Pt were annealed to 600 K to cause clusters of Pt to form, an enhancement in the CO_2 photoformation rate and total yield was not observed. From spectra B to D, the CO_2 photoformation rate and yield decreased as the Pt coverage increased in the clusters formed at 600 K. This indicates that the photooxidation to form CO_2 occurs on the exposed TiO_2 surface, and that the exposed TiO_2 surface area is reduced as the Pt coverage is increased.

The right panel of Figure 9 shows the exponential decay of the CO_2 photoformation rate derived from the data in the left panel of Figure 9. The exponential decay rate for the CO_2 photoformation spectra remains essentially constant for the different coverages of Pt and is essentially the same as for the clean TiO_2(110) surface.

IV. Discussion

A. Pt Metal Deposition and Thermal Behavior on the TiO_2(110) Surface. The combined results of the Auger uptake curve for Pt on the TiO_2(110) surface presented in Figure 1 and the CO thermal desorption studies paint a picture of the morphology of Pt overlayers as a function of deposition at 300 K. The upward concave curvature of the Pt/Ti and Pt/O Auger ratio plots is consistent with Pt deposition, but the growth mode may not be determined from these data. LEIS studies made on a stoichiometric surface indicated that Pt forms 3-D islands before the whole TiO_2(110) surface is covered with Pt.[30] The report states that exposed Ti atoms exist on the surface when up to 3−4 ML of Pt is deposited on the surface. In the present series of studies, CO thermal desorption from Pt is the only thermal desorption process observed at 2 ML of deposited Pt. This observation suggests that there are no Ti sites available for CO adsorption at 2 ML of deposited Pt.

Auger spectroscopy studies of Pt overlayers with an initial coverage of 1.5 ML show a significant change following annealing to temperatures above 300 K. First there is a slow decrease in the Pt/Ti and Pt/O Auger ratio up to 600 K. Above 600 K there is a more rapid decrease in the Auger ratios up to ∼800 K beyond which the Auger ratio remains relatively constant. Since the onset of Pt desorption would not be detected until 1500−1700 K, it is proposed that the decrease in the Auger ratio is due to agglomeration of Pt into 3-D clusters. This structural rearrangement would explain the decrease of the Pt Auger signal due to the self-screening effects of Pt atoms in the clusters.

The CO thermal desorption measurements presented in Figure 4 provide additional support for the proposed formation of clusters and illustrate the structural change that occurs when 0.15 ML of Pt is annealed to 600 K. The CO thermal desorption yield from Pt at ∼460 K decreases by a factor of 2, and the CO thermal desorption yield from TiO_2 at ∼140 K increases by a factor of 2. From the calibrated amount (0.15 ML) of Pt deposited on the TiO_2(110) surface at 300 K, the fraction of Pt-covered TiO_2 surface area is ∼0.09. After clustering at 600 K the surface area of TiO_2 taken up by the Pt clusters is ∼0.04. As the Pt-covered surface is annealed to higher temperatures it has been reported that Ti_xO_y migrates over and encapsulates the Pt clusters eliminating CO adsorption.[28] At temperatures above ∼ 750 K we find evidence for Ti_xO_y encapsulation of the Pt clusters. By sputtering this surface, we showed (Figure 5) that the Pt/Ti Auger ratio initially increased reaching a maximum at a sputtering fluence of 2×10^{15} Ar^+/cm^2. This indicates that Ti_xO_y layers of the order of monolayer thickness are involved in the encapsulation process. The temperature of onset of Ti_xO_y encapsulation (∼750 K) disagrees somewhat with other work[30] where an onset temperature of 450−650 K is reported. This may be due to differences in the manner of measurement of the TiO_2 crystal temperature.

B. Pt Cluster Formation on Defective TiO_2(110). A crude estimate of the average size and spatial distribution of Pt clusters was made following cluster growth at 600 K. It was observed that the Pt(NVV) Auger intensity decreased to 0.81 of the intensity of that of the single monolayer of Pt employed. Two models of cluster shape were employed, namely the growth of hemispherical clusters and the growth of cylindrical clusters. Both models yielded similar estimates of Pt cluster size. The attenuation length of Pt(NVV) Auger electrons has been measured previously as 4.1 Å,[10] and the Pt layer spacing was assumed to be 2.47 Å.

Assuming that all Pt clusters are of the same size, a hemispherical cluster diameter of 16 ± 2 Å was deduced. Each cluster contains ∼90 Pt atoms. If the clusters are uniformly distributed in an assumed hexagonal array, the cluster-center-to-cluster-center distance is ∼28 Å. Since the clusters nucleate

(30) Steinrück, H.-P.; Pesty, F.; Zhang, L.; Madey, T. E. *Phys. Rev. B* **1995**, *51*, 2427. Pesty, F.; Steinrück, H.-P.; Madey, T. E. *Surf. Sci.* **1995**, *339*, 83.

Table 1. Comparison of Kinetics and Yield Parameters for CO_2 in CO Photooxidation on $Pt/TiO_2(110)$

surface condition (after 600 K anneal)	$(dN_{CO_2}/dt)_0$[a] (A)	Y_{CO_2}[b] (A·S)	$(dN_{CO_2}/dt)_0/Y_{CO_2}$
0 ML Pt	$(7.8 \pm 0.07) \times 10^{-10}$	$(8.7 \pm 0.26) \times 10^{-9}$	0.090 ± 0.003
0.15 ML of Pt	$(6.6 \pm 0.07) \times 10^{-10}$	$(6.8 \pm 0.20) \times 10^{-9}$	0.097 ± 0.003
0.5 ML of Pt	$(1.8 \pm 0.06) \times 10^{-10}$	$(2.1 \pm 0.13) \times 10^{-9}$	0.086 ± 0.006
2.0 ML of Pt	$(1.4 \pm 0.06) \times 10^{-10}$	$(1.5 \pm 0.15) \times 10^{-9}$	0.093 ± 0.010

[a] Initial CO_2 production rate. [b] Total CO_2 yield.

on anion vacancy defect sites, the calculated coverage of Pt clusters, 1.6×10^{13} clusters /cm^2, should be equal to or less than the number of vacancy defects (estimated to be $\sim 10^{14}$ defects /cm^2).[17,19]

C. Effect of Pt-Electron Trap Sites on CO Photooxidation. The experimental methods employed here provide a basis for the direct observation of the electronic effect of Pt clusters on the kinetics of the model CO photooxidation reaction. Three types of measurements are possible:

1. Type one is the measurement of the relative rate of CO_2 production at any stage of the reaction. This is accomplished in the fast-pumped UHV mass spectrometer system, since under fast pumping conditions the magnitude of the CO_2 partial pressure observed in a transient experiment is directly proportional to the rate of CO_2 production on the sampled region of the surface, $\Delta P_{CO_2} \propto \Delta N_{CO_2}/dt$.[31,32]

2. Type two is the measurement of the relative yield of CO_2 for the complete reaction. This is accomplished by evaluation of the integral $\int \Delta P_{CO_2}\, dt$ over the time period required for the complete photoreaction experiment.

3. Type three is the measurement of the characteristic first-order decay time, τ, during CO_2 photoproduction as the coverage of CO(a) and O_2(a) decreases. This decay time is proportional to the rate constant for the photochemical reaction assuming that the ratio of the CO(a) and O_2(a) coverages does not change during photooxidation, and that the light intensity is constant.

Measurement methods 1 and 2 are fundamentally connected to the kinetics of the photooxidation reaction and may be employed to ascertain the effect of Pt electron traps on the reaction kinetics. Figure 9 shows the comparison between the photooxidation kinetics on $TiO_2(110)$ containing a preset level of defect sites produced at 600 K (Experiment A) and similar experiments involving $TiO_2(110)$ containing various size clusters of Pt made at 600 K. It is noted that the initial rate of CO_2 photoproduction (judged from the initial peak height of ion current at 48 amu) is not enhanced by Pt clusters produced at various initial Pt coverages. An enhancement in CO_2 production rate would increase the CO_2 initial peak height and decrease the decay time of the photoreaction assuming the initial CO and O_2 coverages and the exposed surface area of the defective $TiO_2(110)$ surface are identical. Such an effect is not seen. Instead a decrease in both the CO_2 peak height and the CO_2 integrated yield is observed at all Pt coverages studied, compared to the clean $TiO_2(110)$ containing the controlled level of surface vacancy defects.

This decrease in initial CO_2 formation rate and CO_2 yield is due to Pt cluster nucleation on defect sites reducing the number of chemisorbed O_2 molecules available for the photooxidation reaction. Table 1, column four, shows that for all levels of Pt cluster sizes and surface densities studied, the initial rate of the photooxidation reaction, $(dN_{CO_2}/dt)_0$, is proportional to the total yield, Y_{CO_2}, of the reaction, showing that the decreases in initial CO_2 formation rate and in CO_2 yield are due to reactant supply effects and not to significant changes in the kinetic rate constant for the reaction.

The constancy of the ratio $(dN_{CO_2}/dt)_0/Y_{CO_2}$ for clean TiO_2 and all Pt cluster deposits is also consistent with the constant CO_2 production decay time, τ, for all Pt deposits shown in the right-hand panel of Figure 9.

The estimated size and spatial distribution of Pt clusters provide the following information relevant to the hypothesized role of Pt electron traps:

1. The Pt clusters are metallic due to their size.

2. The average estimated lateral distance between Pt clusters ($\sim$28 Å) indicates that in the $TiO_2(110)$ surface region, each electron-hole pair must be produced within a distance of $\sim$16 Å or less from the center of a Pt cluster. This distance is of the same magnitude as the correlated electron-hole pair length (10−100 Å) in semiconductors.[33] Thus it is likely that the hypothesized trapping effect at the Pt/TiO_2 Schottky barriers would not be influenced by spatial range effects.

The results on the model $Pt/TiO_2(110)$ photocatalyst may be compared to photocatalytic CO oxidation studies made on a high-area Pt/TiO_2/mortmorillonite clay at 300 K, where a large enhancement in reaction rate was found compared to non-platinized TiO_2.[8] In these studies, the authors postulate that the Pt may either catalyze a *thermal* oxidation process lending to CO_2 formation or act as an electron trap. Our studies, done at low temperatures, are able to show with certainty that Pt on TiO_2 does not involve itself in the electronic excitation processes in the TiO_2, as judged by the reaction kinetics and reaction yield.

These results clearly indicate that Pt clusters derived from deposits of 0.15 to 2 ML of Pt are ineffective in enhancing the rate or yield of chemisorbed CO undergoing photooxidation on $TiO_2(110)$ in experiments carried out at 105 K, where most thermal effects will be quenched. Electron trapping in the Pt either does not occur or is ineffective in enhancing the kinetics of the photochemical process.

These findings are in disagreement with existing views of the role of high work function metals in enhancing the photochemical efficiency of TiO_2 photocatalysts.[1−8] Similar studies of other photooxidation reactions on Pt/TiO_2 are needed in order to clarify in more general terms the role of the electron trapping in photoreactions on TiO_2 photocatalysts.

V. Summary and Conclusions

Platinum overlayers on a $TiO_2(110)$ surface have been studied to determine the structural characteristics and to probe the effect of Pt on the CO photooxidation reaction.

1. Auger spectroscopic and CO thermal desorption measurements have demonstrated that Pt layers are thermally unstable and form 3-D clusters on the $TiO_2(110)$ surface upon heating above $\sim$300 K. Above $\sim$750 K, Ti_xO_y encapsulation of Pt clusters is observed in agreement with other studies.

2. Pt deposition at 300 K titrates the active sites for CO photooxidation and eliminates the process.

3. Pt cluster electron traps on $TiO_2(110)$, if they exist, are ineffective for the enhancement of the CO photooxidation reaction rate or the reaction yield.

Acknowledgment. We gratefully thank the Army Research Office for the support of this research.

JA953601C

(31) Yates, J. T., Jr. *Methods Exp. Phys.* **1985**, *22*, 425.
(32) Redhead, P. A. *Vacuum* **1962**, *12*, 203.
(33) Ulbricht, R. G., In *Materials Science and Technology, Electronic Structure and Properties of Semiconductors*, Cahn, R. W., Haasen, P., Kramer, E. J., Eds.; VCH: Weinheim, 1991; Vol. 4, p 78.